WCTE 2016
World Conference on Timber Engineering
August 22-25, 2016 | Vienna, Austria

AN INNOVATIVE HYBRID TIMBER STRUCTURE IN JAPAN : EXPERIMENTS ON THE LONG TERM BEHAVIOR IN BEAM

Kohei Uchimura[1], Shinichi Shioya[2], Tomoka Hira[3]

ABSTRACT: Hybrid composite glulam timber reinforced using deformed steel bars and epoxy resin adhesive (RGTSB), was significantly developed in Kagoshima University. A long term laboratory investigation on a 4.5-meter-span hybrid timber beam and a non-hybrid timber beam was started from August 2011. The beam was made of RGTSB and another was of conventional glulam timber. Test in early three months promoted creep deflection in the beams, by causing mechano-sorptive creep by humidifying in test room, in order to reveal effects, which the deformed bars suppress deflection in the RGTSB beam. This paper presents the results and observations of the long-term test. The deformed bars was revealed to suppress effectively the flexural creep deformation in timber. Also a simplified calculation method is presented to predict the deflection-time curve of RGTSB beam under long-term loading, using the curve of conventional glulam timber beam. The approximations showed reasonable agreement in the results of the RGTSB beam.

KEYWORDS: Hybrid timber, glulam, glued-in rod, deformed bar, creep, experimental investigation, calculation model

1 INTRODUCTION

Japanese cedar is one of rapid grown species, which was planted much in Japan, 5-6 decades ago. In Japan, there is, at present, a biggest concern about utilizing the cedars as structural glulam products for timber structure. However, most of the cedars are low-grade on stiffness and strength for structural members, due to the rapid growth.

On the other hand, many designers desire innovative timber members and their structural systems for buildings, with slender members such as reinforced concrete or steel members.

One of reinforcement techniques for Japanese cedar's glulam timbers would be using deformed steel bars (deformed bars) and adhesives, which improve flexural stiffness and strength of timber members [1-2].

Shioya, i.e. one of authors, proposed the structural system and the construction for buildings, with Reinforced Glulam Timber Structure system using Steel Bars (RGTSB, nicknamed "Samurai" in Japan); constructed the first prototype building of two-way frame structure using the system in cooperation with Yamasa Mokuzai corp as shown in Figure 1.

RGTSB can be extremely efficient in long-span beams, however, design of the long beams may be governed by serviceability limit states and the deflection under long-term load which is one of the serviceability criteria.

The long-term behaviors of timber beams depend on a number of phenomena such as creep, shrinkage or swelling effects in timber.

On the other hand, creep of steel is extremely little at air temperature, therefore steel bars embedded and bonded in RGTSB would be expected to suppress the flexural creep deflection in the beams. This paper presents results of long-term experimental investigation on RGTSB beam (4.5 meter span), using mechano-sorptive creep.

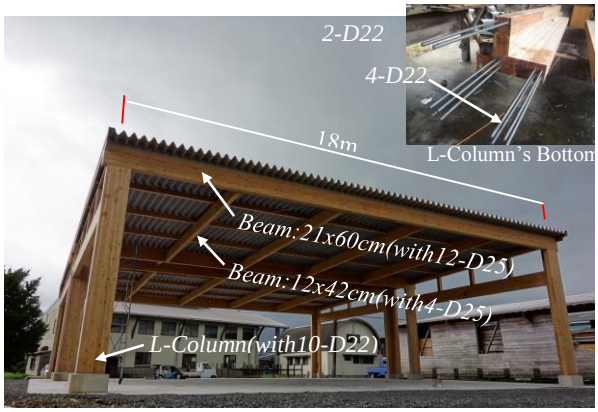

Figure 1: *The first prototype building utilizing RGTSB "Samurai" in 2014*

[1] Kohei Uchimura, the 1st-year Master's degree Student, Department of Architecture and Architectural Engineering, Kagoshima University, Kagoshima, Japan, uchimura@sos.aae.kagoshima-u.ac.jp
[2] Shinichi Shioya, Kagoshima,University ,Japan, shin@aae.kagoshima-u.ac.jp
[3] Tomoka Hira, Naito Architects, Japan

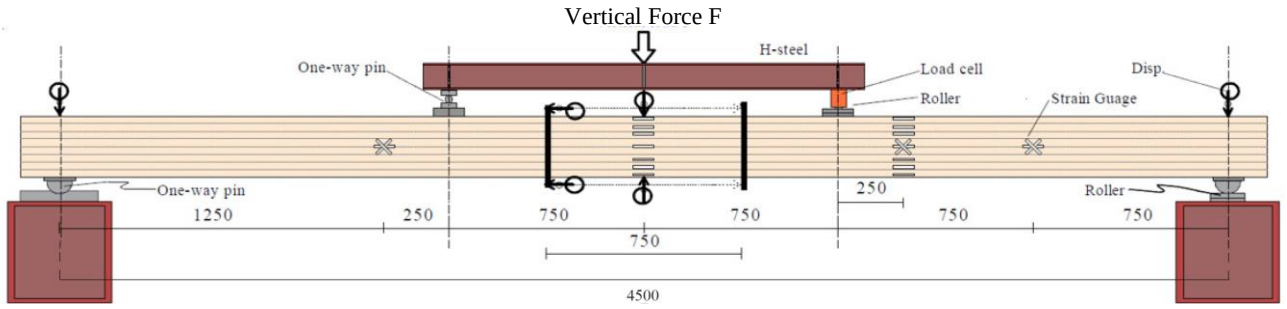

Figure 2(a): *Specimen configuration and set-up*

Table 1: *Material testing - Deformed bar: D16*

Deformed bar（SD295）		
Young's modulus (N/mm^2)	Yield strength (N/mm^2)	Tensile strength (N/mm^2)
1.84×10^5	358	620

Table 2: *Material testing - Glulam timber*

Timber（E65-F255）	
Young's modulus (N/mm^2)	Flexural strength (N/mm^2)
7.77×10^3	52.8

2 BACKGRAND

Several researchers have tried to develop hybrid composite timber [1-6]. M. Kaestner et al. have developed hybrid composite timber beam glued deformed bars and reported the short-term loading experiment on the beams [1]. S. Goto, et al. conducted long-term loading test on timber beams glued deformed bars with epoxy resign adhesive, however they reported the bars would not clarified to suppress the creep deflection [2]. T. Tanner et al. have investigated long-term performance on Timber-Concrete-Composite beam, however, have not proposed the prediction method for creep deformation of them yet [4]. Hoyle et al. [7] conducted creep experiments under conditions of cyclic relative humidity, and found that creep for cycled specimen greatly exceeds creep for un-cycled specimen.

3 EXPERIMENTAL PROGRAM

3.1 MATERIALS

Glulam Timbers were made of Japanese cedar lamellas glued together with resorcinol resin adhesive; the grade of Glulam Timbers was arranged according to E65-F255 (JAS). Deformed bars embedded in timber were SD295 grade; nominal diameter, 16mm.
Adhesive between the bars and the lamellas was two-component liquid epoxy resin.

3.2 SPECIMENS AND SETUP

Two beam specimens were scaled down at ratio of a half and tested in long-term under four-point flexural bending as shown in Figure 2. Figure 3 shows the beam sections. Specimen BN was a conventional glulam timber, and Specimen BR was composed of RGTSB.

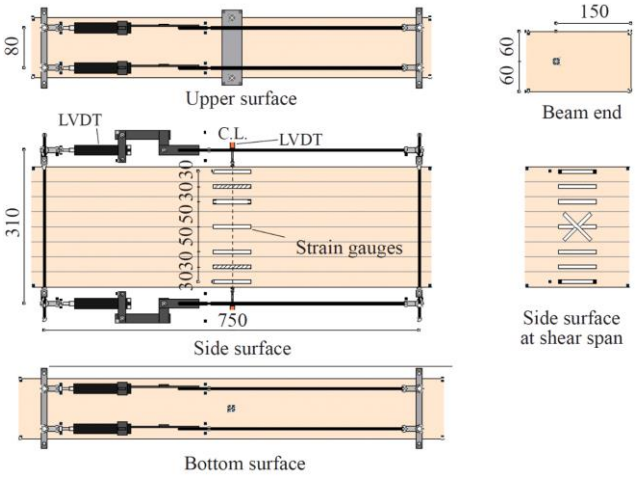

Figure 2(b):*Detail of LVDT set-up*

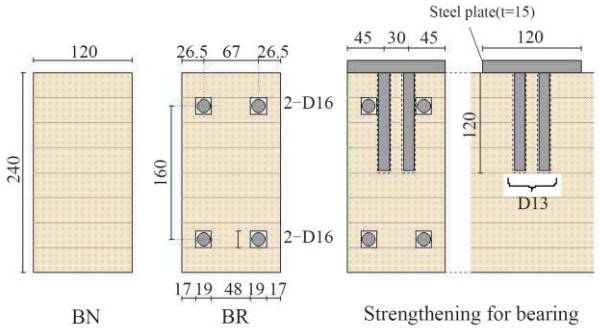

Figure 3: *Specimen cross-section and reinforcement for bearing*

Figure 4: *Vertical loading set up at mid-span, strain gauges, LVDT*

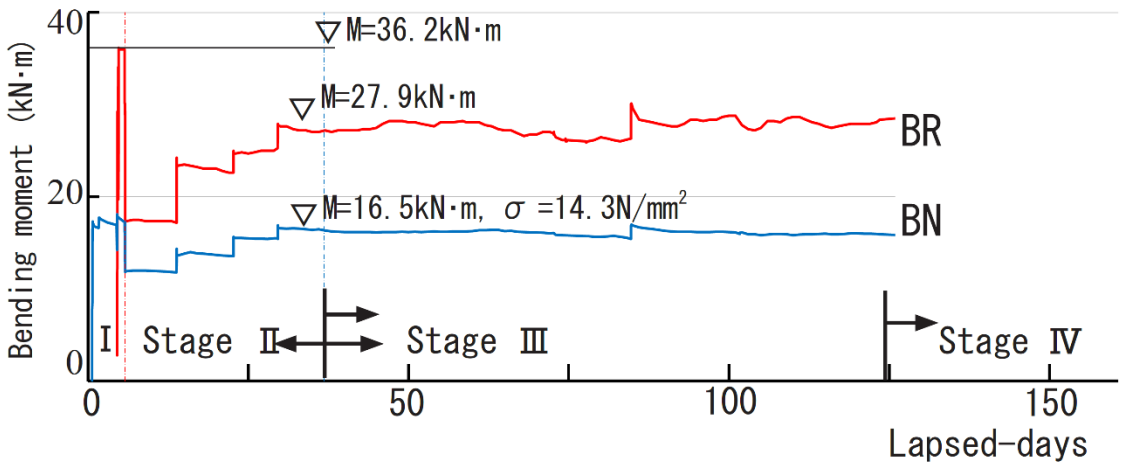

Figure 5: *Loading moment at mid-span – lapsed days*

3.3 LOADINGS

Vertical force F, in Figure 2, was loaded to mid-span of the H-steel on the beams, using principle of lever. The load was controlled monitoring the load-cell (Figure 2). Loading bending moment-lapsed days at mid-span of beam, is showed in Figure 5. The loading was separated up the following four stages as a result, in order to reveal, in early, the effect of the deformed bars suppressing the long-term deflection due to creep. The loading to specimen BN was planned as a standard, based on results of preliminary bending laminar test; Specimen BR was coincided with the specimen BN, on curvature at the mid span.

Stage I : Loading to BN was planned flexural stresses at the mid-span, to be 15N/mm^2: 28.4% of experimental flexural Strength fu; fu=52.8 N/mm^2 in lamellas. Loading to BR was adjusted as curvature at the mid-span to be equalled to that of BN, measured by displacement transducers, however the deformed bar in BR exceeded slightly yield strain. Then, the loading ratio of BN to BR was 1:2.

Stage II : Just after then, un-loadings in both specimens were conducted in order to be long-term behaviour without yielding in BR, and re-loadings were conducted as the following step; to be 15.5% in the 1th; 18.6%, in the 2nd; 20.5%, in the 3rd; 21.5%, in the 4th; adjusting the mid-span curvatures on BN and BR to be same, using average curvatures by the strain-gauges at the mid-span; in the 4th, the loading ratio of BN to BR was 1:1.6. The long-term deflection in both specimens could not be observed clearly until 7 days lapsed in the 4th step.

Stage Ⅲ : In order to boost the deflection using mechano-sorptive effect[7], the humidity in the test room, 2.0x2.0x5.5m room size , was varied from 56% to 84% in RH, by humidifying under stage II-last loading, in the 4th step.

Stage IV : The humidifying was stop on the 120 lapsed day from experiment-start, and lasted under stage II, until July 2015.

3.4 MEASUREMENT

Main recorded data was as follows: vertical load, by load-cell; deflection and bending angle at the mid-span, by displacement transducers; flexural strain and shear strain on timber in the beams, by waterproofing strain-gauges, and longitudinal strains on the deformed bars in BR at the mid-span, by strain gauges; these deflection, angle, and strain were measured on the front side and back side of the specimen in Figure 2b. Relative humidity and temperature in the test room, by devices; moisture content by timber brocks in stage III.

4 RESULTS

4.1 BENDING STRAIN DISRITUTION

Figure 6 shows flexural strain distributions at the mid-span, which were measured at both front side and back side in Figure 2b, respectively; in BR specimen, also strains of top and bottom bars. Open marks are on timber; solid marks are on the deformed bars embedded in BR in Figure6

The followings are found.

At initial loading in the stage I;

Figure 6a indicates the distributions at bending moment, 15.4kN･m in BN, 23.1kN･m in BR at mid-span, on the first day. The distributions on timber were approximately line; in BR, the strains on deformed bars were nearly 20% greater than them on timber.

At long-term loading in the stage III;

Figure 6b indicates them at 15.9kN･m in BN, at 28.2kN･m in BR, on the 112 days. The distributions on timber were also linear; the strains on the bars were nearly equal to the timber. Figure 6c shows changes form Figure 6a to 6b: the changes were nearly equal to line.

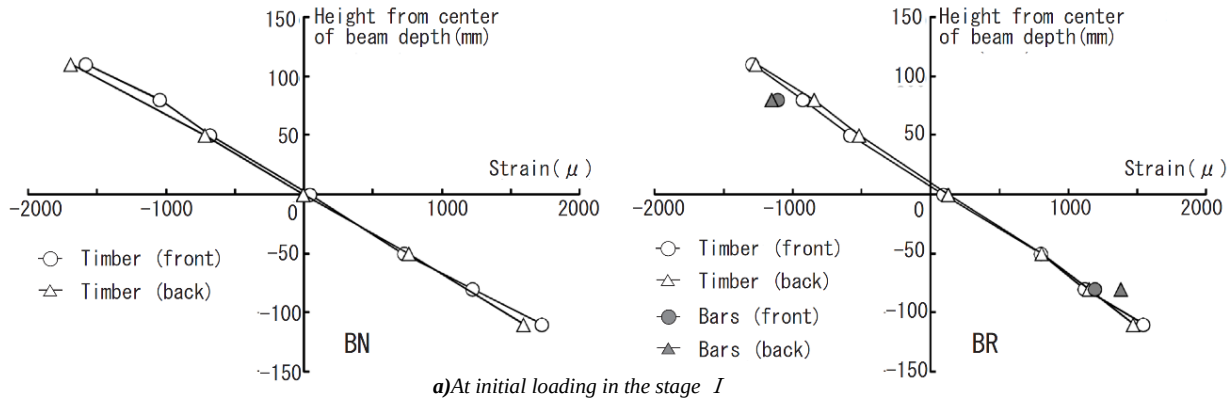

a)*At initial loading in the stage I*

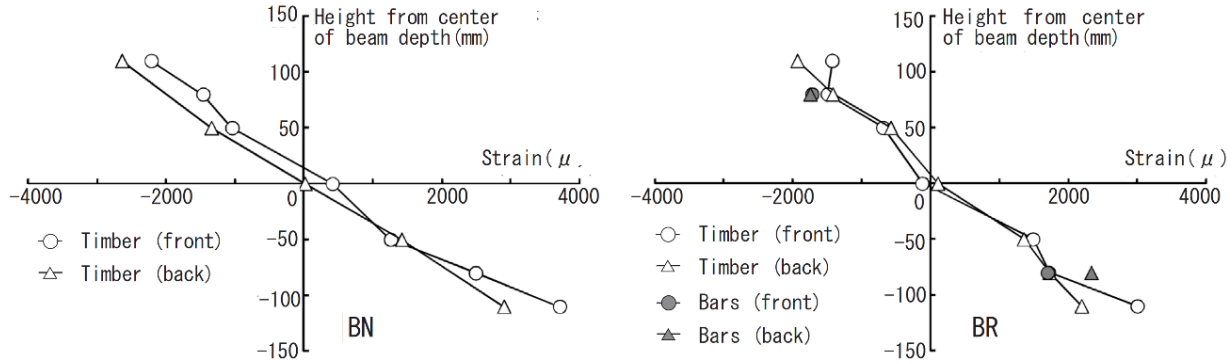

b)*At long-term loading in the stage III*

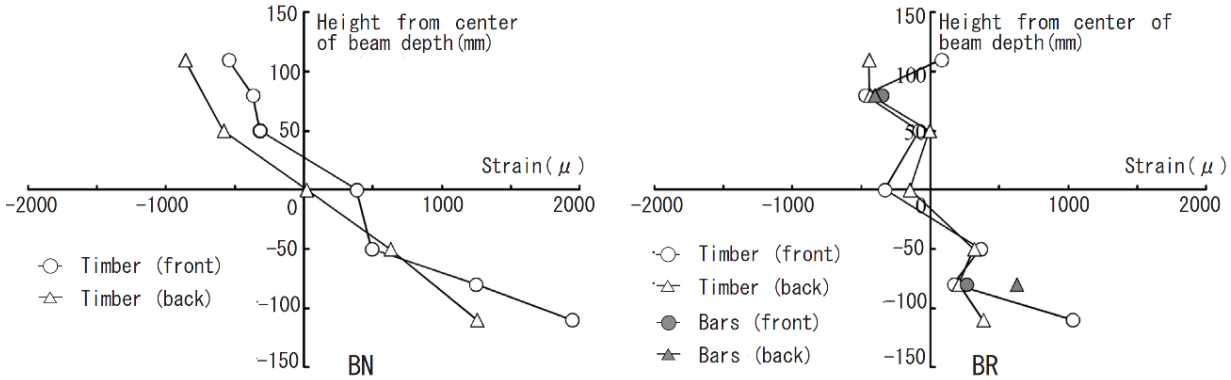

c)*Changes from Figure 6a to Figure 6b*

Figure 6: *Flexural strain distributions in cross sections at mid-span*

4.2 BENDING MOMENT- CURVATURE CURVES

Figure 7a shows bending moment- curvature curve at mid-span in the stage I, using the strain-gauge curvature: solid lines indicate experimental results; blue dot-dash line, elastic-stiffness experimental result for BN; red dot-dash line, stiffness obtained by adding a calculated increase due to reinforcing bars to the blue line stiffness. The red dot-dash line stiffness could predict the stiffness of BR with over 10% error.

Figure 7b shows the bending moment- curvature curves in term from stage I through III; Figure 8 shows the curvature-lapsed days; Figure 9 shows changes in relative humidity, moisture content and temperature. It was noted clearly that the curvature in BN, non-reinforced, increased at beginning of the stage III, humidified, however that of BR, reinforced, did not increase much, although bending moment of BR was 1.7 times of that of BN.

Some small changes in the stage III on the curve were caused by adjusting the level of lever arms with long-term deflection increasing.

These data reveal that the deformed bars glued in RGTSB can diminish extremely the long-term deflection in timber beams.

4.3 MID-SPAN DEFLECTION.

Figure 10 shows deflection-lapsed days at the mid-span, measured at upper surface and bottom surface of the specimens, respectively; solid lines indicate the upper; dot lines, the lower. Difference between the upper and the lower began to occur at the beginning in stage III, at each specimen, due to swelling effect [8], with increasing moisture content in timber blocks in Figure 9

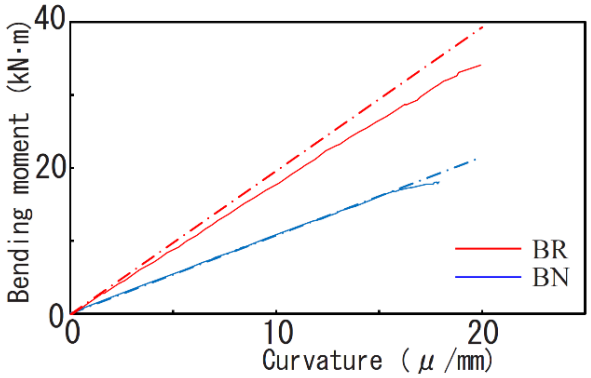

a): *At initial elastic loading in stage 1*

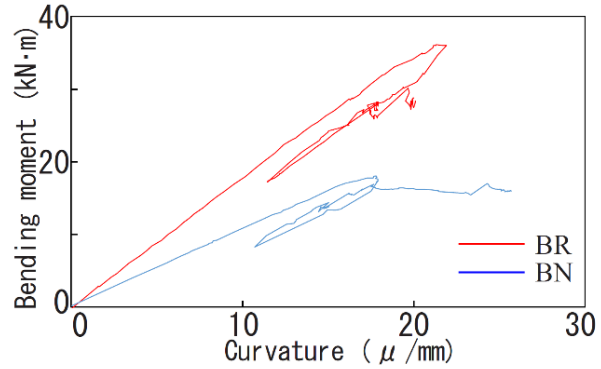

b): *From stage 1 until stage Ⅲ*

Figure 7: *Bending moment-curvature at mid-span*

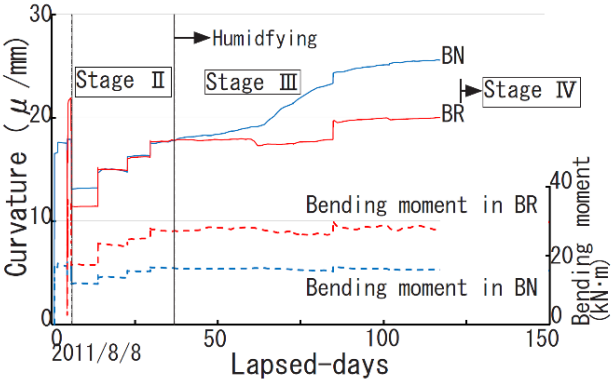

Figure 8: *Curvature – lapsed days at mid-span*

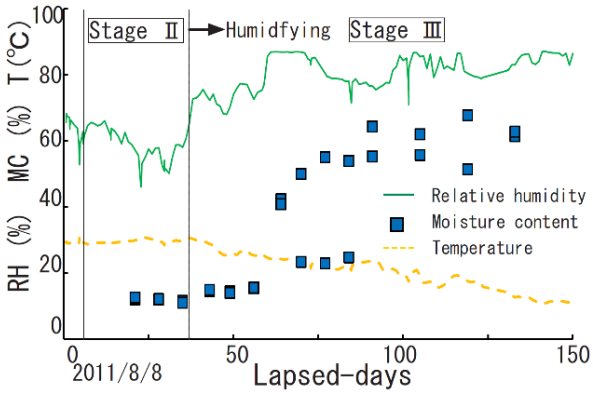

Figure 9: *Changes in relative humidity, moisture and temperature*

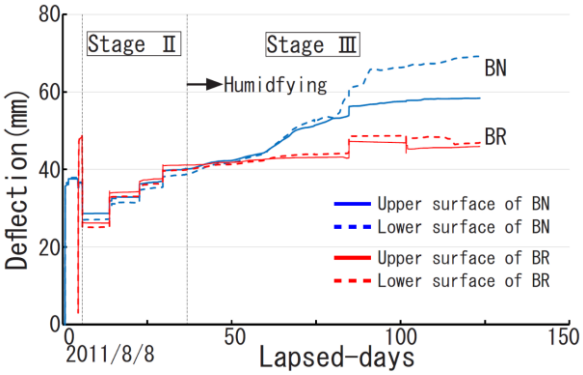

Figure 10: *Deflection-lapsed days at mid-pan*

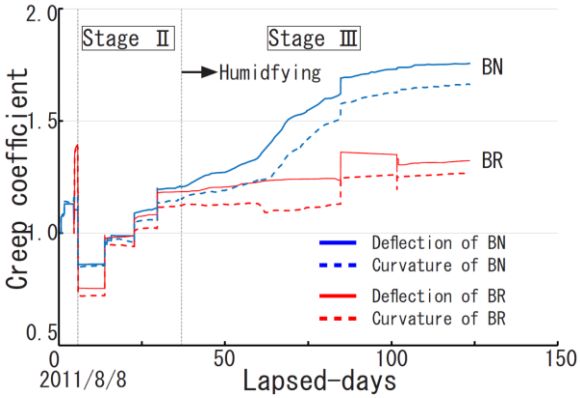

Figure 11: *Creep coefficient-lapsed days: curvature and deflection at mid-span*

4.4 CREEP COOFFICIENTS

Figure 11 shows creep coefficient-lapsed days of the curvature and the deflection to compare them; solid lines indicate them of the deflection; doted lines, the curvature. Initial elastic curvature and deflection were assumed to be them measured in stage I corresponding to loading at the beginning in stage III. The deflection creep is more than the curvature creep, because, we think, the deflection includes shear deformation at ranges except the min-span and bearing deformation at loading point in the timber.

5 PREDICTION FOR CREEPS

5.1 CONCEPTION FOR CALUCULATION

Imaging that a mechanical model composed of a wooden uni-axis spring and a steel uni-axis spring resist to constant Force F such as an weight, without rotating as shown in Figure 12a, deflection, δo, corresponding to F is expressed as follows:

$$\delta_0 = \frac{F}{(K_W + K_s)} \qquad (1)$$

where Kw is spring constant of the wooden spring; Ks is spring constant of the steel spring.

In above, compatibility of deformation between the wooden spring and the steel spring is assumed.

Furthermore, assuming that Kw degrades due to creep, and the reduction coefficient, αt, of Kw decreases with increasing the loading period, t, the deflection, δt, at the period t, is expressed as follows:

$$\delta_t = \frac{F}{(at \cdot K_W + K_S)} \tag{2}$$

In these situation, the creep coefficient, ϕ, can be defined as follows:

$$\Phi = \frac{\delta_t}{\delta_0} = \frac{(K_W + K_S)}{(at \cdot K_W + K_S)} \tag{3}$$

$$= \frac{\left(1 + \frac{K_S}{K_W}\right)}{\left(at + \frac{K_S}{K_W}\right)} \tag{4}$$

In the above, Equation 4 was derived using the uni-axis spring model. The creep coefficient, Φb, for two elements resisting to bending moment as shown in Figure 12b, also, can be derived by using EIw and EIs in place of Kw and Ks in Equation 4, as follows:

$$\Phi_b = \frac{\left(1 + \frac{EI_S}{EI_W}\right)}{\left(at + \frac{EI_S}{EI_W}\right)} \tag{5}$$

where EIw is the initial flexural stiffness of the wooden element; EIs is the initial flexural stiffness of the steel element; α t is the reduction coefficient to EIw due to long-term loading; α t is less than 1.0.
Equation 4 indicates that the creep coefficients, Φb, decrease gradually toward 1.0 with EIs/EIw increasing: Φb is 1.0,i.e. no creep. If bond stiffness and bond strength between the deformed bars and lamellas are extremely sufficient, the deformed bar can suppress the flexural creep deformation in RGTSB beam, corresponding to the amount of the bars. We have already reported that both bond stiffness and bond strength using epoxy resin adhesive are sufficiently to design RGTSB beams for shear force, based on bar-slip test in lamella or glulam timber blocks [9] and Navier hypothesis is effective in RGTSB members [10].

5.2 IMPLEMENTATION AND COMPARISION

Long-term curvature-lapsed days curve in BR, was calculated as follows:
1) curvature at lapsed days was equal to the product of the initial curvature and Φb by Equation 5; 2) EIs was the flexural stiffness of the deformed bars calculated in beam section, the product of the inertial moment of the bars to the neutral axis in beam and Young's modulus of the bars; 3) EIw was flexural stiffness of timber in the beam, measured experimentally in BN, non-reinforced; 4) αt was inverse of wooden creep coefficient on curvature Φw, measured experimentally in BN in Figure 11

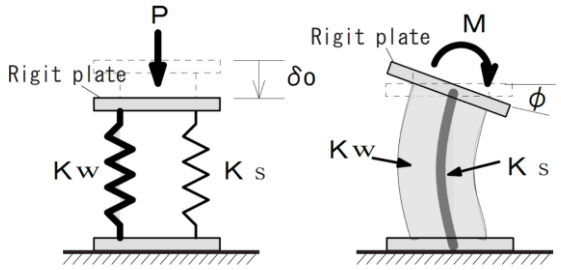

a) *Axial springs* ***b)*** *Flexural springs*

Figure 12: *Mechanical springs models for calculation for creep coefficient in RGTSB beams*

Figure 13 shows comparison of Long-term curvature-lapsed days at mid-spam in BR: Red line is calculation; broken line is experiment, removed the influence of deformed bars yielding plastic strains in stage I, in Sec. 3.3. The calculation has approximated the experimental result. Equation 5 is referred to be able to predict the effect of deformed bars suppressing the flexural creep deflection in RGTSB beam, by selecting appropriately creep coefficient of timber in the beams.

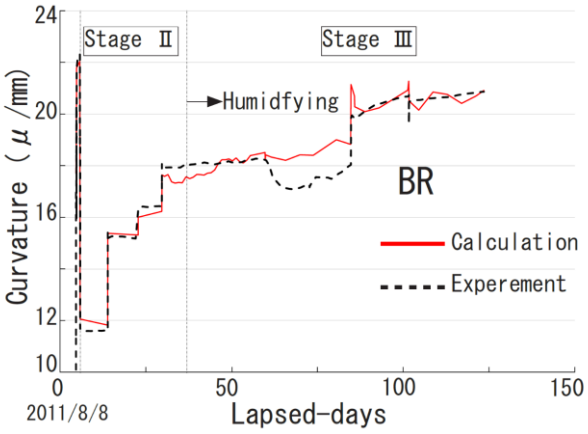

Figure 13: *Comparison between experiment and calculation on flexure curvature - lapsed days at mid-span in BR*

5.3 CREEP COEFFICENT WITH STEEL RATIO

Deflection in conventional timber beams increases under long-term loading; the creep coefficient, Φw, is generally set a value from 2.0 or 3.0 according to environmental conditions in design. The deflection increases by the creep, however, RGTSB increases flexural stiffness of the beams and suppresses the creep. This suggests that the long-term deflection in RGTSB beam, δ_{RG}, can be significantly minimized to conventional beam .

Figure 14 shows flexural creep coefficients, *Φb*, calculated by Equation 5, with steel ratio increasing in RGTSB beam, such as beam section shown in Figure 15: the creep coefficient of timber, *Φw*, is 2.0 i.e. αt, 0.5 or 3.0 i.e. αt, 0.33; ratio of Young's modulus in deformed bar to timber, n, is 19.5 or 31.5, these indicate ratio of steel to Douglas pine or Japanese cedar; *pt* or pc indicates ratio of the top or bottom bar area to beam section.

The creep coefficients, *Φb*, decrease gradually toward constant values with *pt*, *pc* increasing, respectively. The coefficient at *pt*, *pc*=2.0% in case that n was 31.5, was minimized to 1.14 for Φw =2.0; 1.31 for 3.0.

5.4 INCREASE OF ELASTIC－FLEXURAL STIFFNESS IN RGTSB BEAM

Basic-calculation method for reinforce concrete members can predict easily and concisely the flexural stiffness of RGTSB beam, with Navier hypothesis and modulus of materials: timbers and deformed bars. This is because timber tensile strength is extremely greater than the compression; no crack occurs until near the ultimate in beam, never seen in concrete.

Figure 16 shows increasing ratio, *λe*, of elastic-flexural stiffness without long-term as increasing *pt* and *pc*, in the beam section in Figure 15; *pt*, *pc* and *n* are same as described in Sec. 5.3. The ratio λe is found to increase proportional to *pt* and *pc*. The timber with n greater than others indicates to be lower-grade than others. The lower-grade of timber in RGTSB beam is, the more flexural stiffness of the beam is referred to increase effectively with *pt* and *pc* increasing.

5.5 LONG-TERM FLEXURAL STIFFNESS IN RGTSB BEAM

Conventional glulam timbers degrade their stiffness themselves under long-term loading. Figure 17 shows decreasing ratios of δ_{RGT} to δo with steel ratio *pt* and *pc* increasing; δ_{RGT} indicates deflection in the RGTSB beam under long term loading; δo, initial elastic deflection in the conventional timber beam with same depth and width in the RGTSB beam; δ_{RGT} / δo are calculated using Equation 5 , considering the effect in elastic of reinforcing bars in Figure 15 and the only flexural deformations; Φw and *n* were assumed in Figure 17. The ratio at *pt*, *pc*=2.0% indicated 0.28: the deflection in RGTSB beams under long-term loading was suppressed to 28% of the initial elastic deflection in the conventional beam. Figure 18 shows increasing ratios of RGTSB beam to the conventional beam on flexural stiffness under long-term loading. The ratio at *pt*, *pc*=2.5% applied in the first building in Figure 1 indicate 7.7; this suggests that depth in RGTSB beams would be designed to nearly half of the conventional timber beam.

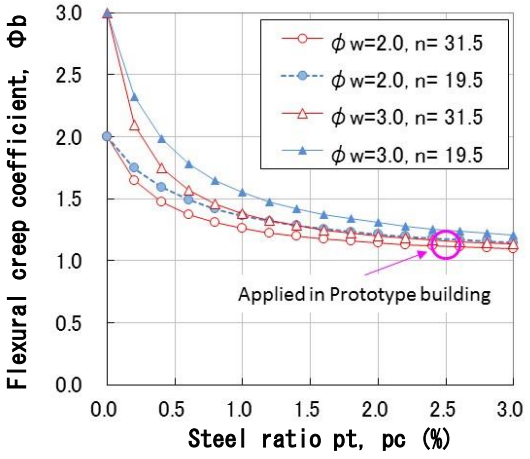

Figure 14: *Flexural creep coefficients, Φb, with steel ratio increasing in RGTSB beams*

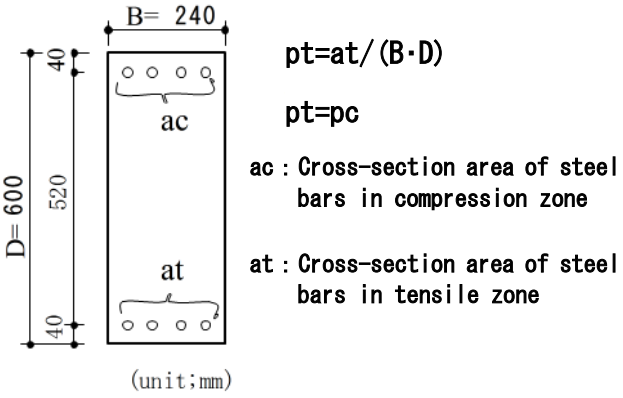

Figure 15: *Example beam section for calculation of creeps, flexural stiffness in RGTSB beam*

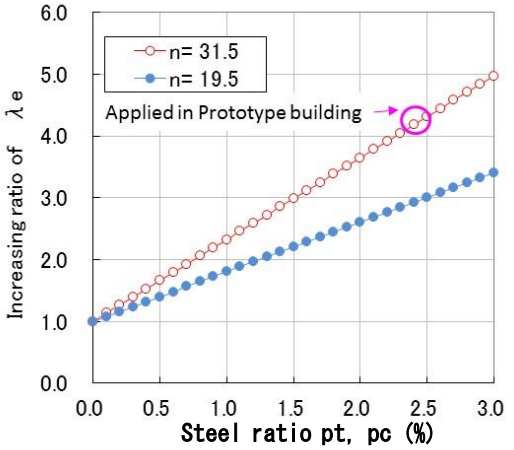

Figure 16: *Increasing ratio of elastic-flexural stiffness, λe, without long-term in loading RGTSB beams*

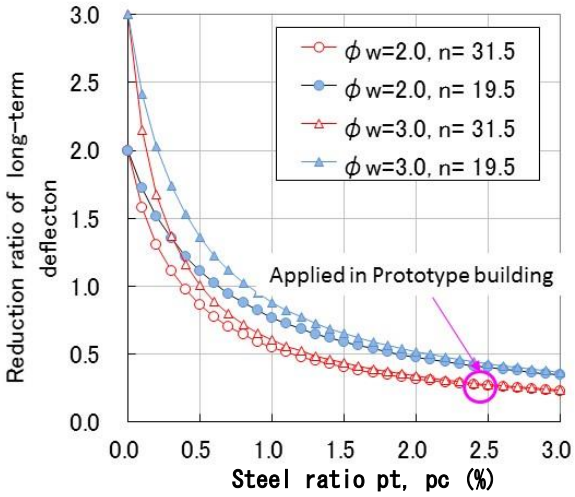

Figure 17: *Reduction ratios of flexural deflection including creep influence with steel ratio increasing in RGTSB beams*

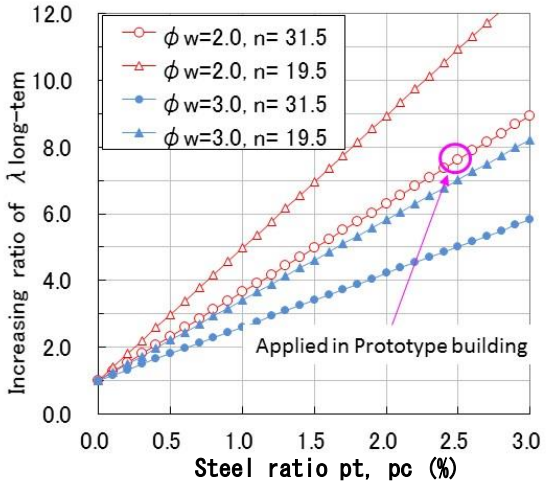

Figure 18: *Increasing ratios of RGTSB beams to conventional timber beams on flexural stiffness, under long-term loading*

6 CONCLUSIONS

The paper presented long-term experimental investigation on hybrid composite reinforced glulam timber (RGTSB) beam.

From this research, it was verified that:

1) using mechano-sorptive effect was extremely available to reveal creep characteristic of hybrid-composite timber RGTSB under long-term loading;
2) reinforcing deformed bars glued in RGTSB suppressed flexural deflection under long term loading: the creep coefficient of RGTSB beam was 1.27 when that of conventional glulam timber was 1.72, under test in this paper;
3) prediction method for flexural creep coefficient of RGTSB beam was proposed, and the calculation by it predicted fairy good the experimental results;
4) flexural creep coefficient of RGTSB beam was found to converge a value decreasing, by increasing steel ratio in the member, based on calculation by the method.

ACKNOWKEGEMENTS

The experimental campaign was funded by LIXLIL foundation and Kagoshima-pre.

The technical support of Takesi Arima is also gratefully acknowledged.

REFFERENCES

[1] M. Kaestner, W. Haedicke, M. Jahreis,K. Rautenstrauch: High-tec timber beam–a high performance properties. In: Proceedings of the World Conference on Timber Engineering WCTE 2014, Quebec City,Canada, 2014.

[2]S. Goto, M. Tokuda, T. Uchizako: Creep of hybrid composite timber beam, The 47th Annual Meeting of the JWRS, No.4915:196, 1997 (in Japanese).

[3]N. Yamad, S. Shioya: Reinforced Timber Assemblies by Reinforcing Steel Bar, AIJ Kyushu Chapter Architectural Research Meeting, No.49:613-616, March 2010 (in Japanese).

[4] E. McConnell, D. McPolin, S. Taylor: Development of novel post-tensioned glulam timber composites, In: Proceedings of the World Conference on Timber Engineering WCTE 2014, Quebec City, Canada, 2014.

[5] W. Winter, K. Tavoussi, T. Pixner, F. R. Parada: Timber-steel hybrid beams for multi-storey buildings: design criteria, calculation and tests, In: Proceedings of the World Conference on Timber Engineering WCTE 2014, Quebec City, Canada, 2014.

[6] T. Tannert, M. Brunner, T. Vallee, Bryn Endacott: Long-term performance of adhesive bonded timber-concrete-composites, In: Proceedings of the World Conference on Timber Engineering WCTE 2014, Quebec City, Canada, 2014.

[7] Hoyle J.R., Jr. Rafik, Y. Itani and J. Jeckard: Creep of Douglas fir beams due to cyclic humidity fluctuations. Wood and Fibre Sci., 18(3):468-477, 1986.

[8] W. Winter, K. Tavoussi, T. Pixner, F. R. Parada: Long-term experimental investigation of timber composite beams in cyclic humidity conditions, In: Proceedings of the World Conference on Timber Engineering WCTE 2014, Quebec City, Canada, 2014.

[9] E. Tomiyoshi, S. SHIOYA et al.: Reinforced Laminated Lumber Structure (R.L.L.S.) with Steel Bar; Part Ⅱ. Experiments of Pushing Steel Bar in Lumber and Adhessive Properties between Steel Bar and Lumber, AIJ Kyushu Chapter Architectural Research Meeting, No.54:773-776, March 2015 (in Japanese).

[10] H. Yagi, S. SHIOYA et al.: Reinforced Laminated Lumber Structure (R.L.L.S.) with Steel Bar Part Ⅲ. Shear Stiffness and Strength on Slab-Beam with L. S.Bolt, s, AIJ Kyushu Chapter Architectural Research Meeting, No.54:777-780, March 2015 (in Japanese).